2020 12th International Symposium on Communication Systems, Networks and Digital Signal Processing (CSNDSP)

Metamaterial-inspired Flat-Antenna Design for 5G Small-cell Base-Stations Operating at 3.6 GHz

João R. Reis*†‡, Mário Vala*†, Telmo R. Fernandes*†, and Rafael F. S. Caldeirinha*†
*Instituto de Telecomunicações, Leiria, Portugal
†Polytechnique of Leiria, Portugal
‡Email: joao.reis@ipleiria.pt

***Abstract*—In this paper, a flat-beamsteering antenna for 5G applications is being presented. The antenna, designed to operate at 3.6 GHz (5G new radio (NR) frequency range 1 (FR1) band n78), presents a unique flat form factor which allows easy deployment and low visual impact in 5G dense scenarios. The antenna presents a multi-layer structure where a metamaterial inspired transmitarray enables the two-dimensional (2D) beamsteering, and an array of microstrip patch antennas is utilised as RF source. The use of metamaterials for beamsteering control allows for the reduction of costly and complex phase-shifter networks by using discrete capacitor diodes to control the transmission phase-shifting and subsequently, the direction of the steering. According to simulations, the proposed antenna presents 13.9 dBi of gain, 100 MHz of bandwidth with a maximum steering range of $\pm$20 degrees, achievable in both elevation and azimuth planes, independently.**

***Index Terms*—5G, antenna, base-station, beamsteering, hidden-antenna, metamaterial, frequency selective surface.**

I. Introduction

The 5th generation of mobile network (5G) has been the focus of research in the past few years. The main concept of 5G is to provide a highly flexible and scalable network technology for connecting everyone and everything, everywhere [1].

To date, many 5G systems are already being deployed worldwide, at the same time that the second phase of 3GPP 5G specifications are being standardised, with Release-16 scheduled to be completed by March 2020 [1]. Thus, to comply with requirements of Enhanced Mobile Broadband (eMBB), Ultra Reliable Low Latency Communications (URLLC) and Massive Machine Type Communications (mMTC) (5G use cases [1]), and to cope with the associated growth of users and devices, the reduction of the coverage area (cell size) and the implementation of pico-cells is a trend in 5G [2].

However, the major issue associated with the reduction of covering areas is the consequent increase of cell number (to cover the same area) and thus, the excessive physical deployment of base station (or access point) antennas [2], causing a huge visual impact [3] particularly in dense urban locations. This leads to a high demand for hidden/ concealed antennas with enclosures that allow for the reduction of the visual impact of such massive antenna deployment, *e.g.* antennas embedded in lump poles, fake trees or masked in building facade.

In an antenna engineering perspective, two major fronts are being tackled when designing 5G antennae: *i)* antenna for (mobile) user equipment, which aim at the design of miniaturised antennae, whilst enabling multiple frequencies of operation, multiple-input multiple-output (MIMO) for enhanced signal processing and beamsteering, [4]–[7]; *ii)* the design of novel smart small-cell base station and access point antennas [8]–[10] that should enable, besides massive MIMO, beamsteering to aim at specific directions in time and space, while keeping moderate sizes and appellative shapes.

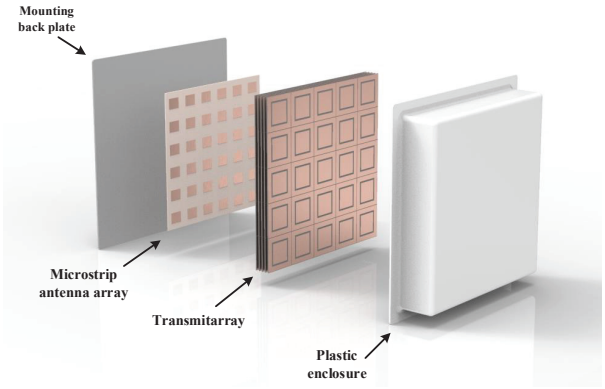

Fig. 1: Overall schematic of the proposed 5G antenna design.

With this mindset, this paper presents a new concept for a metamaterial-inspired flat-antenna design for 5G small-cell base station, operating in the 5G new radio (NR) frequency range 1 (FR1) band n78, with beamsteering capability. The proposed antenna design, depicted in Fig.1, presents a stacked layer design of a microstrip patch array with a transmitarray structure already presented by the authors in [11]–[13]. The transmitarray, seen as the core of this antenna design, is composed of square-slot resonating unit-cells loaded with capacitor diodes, capable of achieving $\pm 20^{\circ}$ of beamsteering, in the two main antenna planes. Due to its the compact and light-weight format, the proposed antenna design is sought as a possible solution to a base station antenna when applied in a ceiling or in a building facade without visually compromising the surroundings.

This paper is organised as follows: section II presents the physical layout of the proposed antenna, while section III introduces the mode of operation of proposed antenna while specifying the details to enable beamsteering. Subsequently, in section IV, the simulation results obtained on the transmitarray antenna are being presented, followed by a critical

978-1-7281-6743-5/20/$31.00 ©2020 IEEE

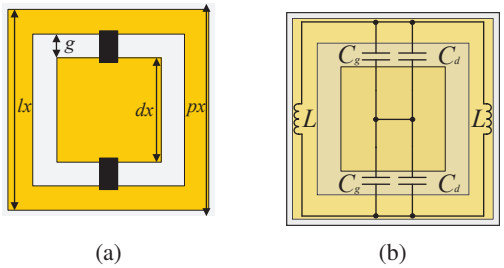

(a) (b)

Fig. 2: (a) Stacked unit-cell and (b) equivalent circuit.

TABLE I: Transmitarray design parameters for the operating frequency set at 3.6 GHz.

Unit-cell dimensions		*Nelco NX9250 substrate*	
Parameter	*Value (mm)*	*Parameter*	*Value*
dx	36		
lx	59.04	ϵ_r	2.5
px	60.04	tan(δ)	0.0017
gx	3	thickness	1.575 mm
layer separation	5		

discussion. Finally in section V, conclusions of the developed work are presented.

II. Proposed antenna design

The antenna design being proposed in this paper is depicted in Fig. 1. The antenna is composed of three main parts: i) a microstrip patch antenna array operating as a feeding source; ii) a transmitarray structure to control the wave front direction and thus, enable beamsteering and, finally iii) a plastic enclosure to cover all electronic parts and provide a clean design and application. Each part is thoroughly detailed in this section.

The microstrip array, composed of a 6×6 elements, has been designed following the recommendations of [14], [15] and assisted by the array design tool provided by CST Microwave Studio (MWS). A probe fed microstrip patch antenna has been used as unitary element of the array. After a complete set of simulation and subsequent optimisation in CST, the 6×6 array with patch dimensions of 23.9×19 mm^2, separated by 41.6 mm ($\lambda/2$ at 3.6 GHz) in both horizontal and vertical direction, printed over a FR4 substrate ($\epsilon_r = 4.4$ and tanδ = 0.025), presents a resonant frequency centred at 3.6 GHz, a bandwidth of 130 MHz and total gain of 18 dBi. For the sake of demonstration, an ideal feeding network has been considered, by forcing a simultaneous multi-port excitation with the same amplitude and phase in each array element, in the simulation environment.

The transmitarray, already presented by the authors in [11]–[13] at various frequencies, has been re-designed and optimised to operate at 3.6 GHz. The transmitarray follows a stacked layer design of square-slot resonating unit-cells loaded with capacitor diodes, as depicted in Fig. 2. The square-slot cell exhibits a band-pass filtering characteristic operating as a frequency selective surface (FSS), which both central frequency and transmission phase-shift are controlled, on-the-fly, by the modifying the value of discrete capacitors placed between the inner patch and outer ring (Fig. 2). Thus, any vertically polarised (TE) incident wave that impinges the transmitarray structure, is re-transmitted with a specific direction defined by the amount of phase delay introduced by each transmitarray element, operating very similar to planar antenna phased array [14].

In particular, a transmitarray element composed of 5 stacked layers of the unit-cell represented in Fig. 2, with dimensions and substrate detailed in Table I, presents the filtering and transmission phase response illustrated in Fig. 3, when the capacitance range is varied from 0.7 to 2.8 pF.In this work, ideal capacitors have been considered and the typical impairments associated to its parasitic effects, i.e. series resistance and inductance have been neglected. The stacking of FSS layers, herein set at 5 layers separated by 5mm, is a well-known method to increase the overall transmission phase shifting (and the order of the spatial filter), as well reported in the literature [16]. This technique is being used herein to enable antenna beamsteering, which principle is thoroughly described in Section III.

According to simulations, the optimum transmitarray element configuration (i.e. 5 layers separated by 5mm) exhibits an effective bandwidth of 100 MHz centred at 3.6 GHz (Fig. 3a), defined by the maximum and minimum cut-off frequency of the lower and higher capacitor values, respectively. The ideal number of layers was achieved by running an extensive parametric simulation in CST MWS, and by analyzing the overall phase-shift between the first and last stacked element. The parametric was set to run for several number of layers and layers spacing, within the considered capacitance sweep range (as in Fig. 3). The global insertion loss for the proposed configuration is better than 4 dB, for every filtering configuration within the unit-cell bandwidth. The relative transmission phase-shift is of $420°$, within the capacitance sweep range (defined from 0.7 to 2.8 pF), respecting therefore the minimum requirement of $360°$ to obtain full control of the beamsteering, as reported in [11].

Note that the transmitarray layers where deliberately designed in a higher performance substrate (Nelco NX9250), when comparing with the one utilised in the feeding antenna (FR4). If FR4 was considered in the transmitarray, the global insertion loss would be much higher (simulated of about 8.5 dB), due to the dielectric properties of the substrate and due to the number of stacked layers. This impact is not as critical in the feeding antenna and a cost-efficiency trade-off must be taken into consideration when selecting the substrates.

In the final antenna configuration, the transmitarray and the microstrip array are separated by 20mm and, protected with by a 3mm thick low-loss plastic enclosure, which confers to the proposed design an overall dimension of $350 \times 350 \times 60$mm^2. While the spacers and the enclosure material have not been considered in the presented simulations, in a practical implementation these can be implemented with low-loss dielectric material, such as PTFE ($\epsilon_r = 2.1, tan\delta = 0.0002$), at the expense of minimally increasing of the excess loss. Several

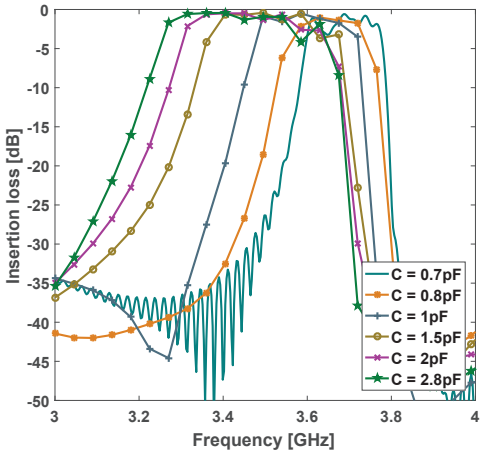

(a)

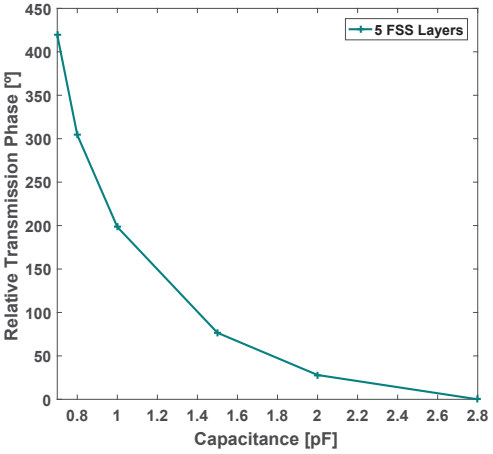

(b)

Fig. 3: (a) Simulated S_{21} and (b) relative transmission phase depending on inserted capacitance.

other technical difficulties could be found when designing and implementing of a feeding network, in the case of using varactor diodes to electronically perform beamsteering. Nevertheless, the authors have successfully demonstrated in [12], a practical implementation of an electronically reconfigurable transmitarray operating at 5.2GHz, whose beamsteering controller and feeding line designs can be directly incorporated in the current design.

III. Enabling 2D beamsteering with a transmitarray

The method of implementing beamsteering with a transmitarray is well detailed in the literature, and particularly in the authors past publication [11], [12]. In fact, it is built on the theory of planar antenna arrays [14], [15], where a progressive phase-shift between adjacent elements should occur along the X and Y directions of a $M \times N$ array so 2D beamsteering could be enabled. Thus, when an incident EM wave impinges a $M \times N$ transmitarray structure, it suffers a punctual phase-delay $\alpha_{m,n}$ in every array element, causing the resultant (re-transmitted) wave to be steered in direction.

As demonstrated in [11], the relation between the two dimensional output directions (Azimuth and Elevation) of the steering angle, and the progressive phase-delay in the transmitarray, is given by (1),

$$\begin{cases} \psi_x = -k_0.p.cos(El).sin(Az) \\ \\ \psi_y = -k_0.p.sin(El) \end{cases}, \tag{1}$$

where ψ_x and ψ_y are the progressive phase along X and Y axis, respectively, and p is the periodicity of the $p \times p$ array elements. This can be represented in a by a relative phase matrix distribution, as in (2),

$$\begin{array}{c} \\ \psi_y \downarrow \end{array} \begin{array}{c} \longrightarrow \psi_x \\ \begin{bmatrix} \alpha_{1,1} & .. & .. & .. & .. & \alpha_{1,n} \\ .. & .. & .. & .. & .. & .. \\ .. & .. & .. & .. & .. & .. \\ \alpha_{m,1} & .. & .. & .. & .. & \alpha_{m,n} \end{bmatrix} \end{array} \tag{2}$$

where $\alpha_{m,n}$ is the phase delay introduced by each individual (m,n) element of the $M \times N$ transmitarray. Thus, for the transmitarray presented in this paper, the unitary phase delay of a specific output angle can then be related to the transmission phase-shift of the transmitarray element (Fig. 3b), and consequently to a specific capacitance value.

For example, in (3) and (4) are represented both phase and capacitance matrices, respectively, of a 5×5 transmitarray composed of the 5 stacked layers of the unit-cell represented in Fig. 2, when beamsteering is set to aim at (10°,0°) (Azimuth,Elevation). These matrices have been obtained with the aid of a Matlab script that computes a phase a capacitance matrix using (1), for every requested output angle and afterwards, converted into capacitance by performing an interpolation between the relative phase matrix (3) and the simulated relative transmission phase curve of Fig. 3b.

$$|\psi_{x,y}| = \begin{bmatrix} 180.28 & 135.21 & 90.14 & 45.07 & 0 \\ 180.28 & 135.21 & 90.14 & 45.07 & 0 \\ 180.28 & 135.21 & 90.14 & 45.07 & 0 \\ 180.28 & 135.21 & 90.14 & 45.07 & 0 \\ 180.28 & 135.21 & 90.14 & 45.07 & 0 \end{bmatrix} \quad [^\circ] \tag{3}$$

$$C_{x,y} = \begin{bmatrix} 1.07 & 1.26 & 1.44 & 1.82 & 2.80 \\ 1.07 & 1.26 & 1.44 & 1.82 & 2.80 \\ 1.07 & 1.26 & 1.44 & 1.82 & 2.80 \\ 1.07 & 1.26 & 1.44 & 1.82 & 2.80 \\ 1.07 & 1.26 & 1.44 & 1.82 & 2.80 \end{bmatrix} \quad [pF] \tag{4}$$

IV. Simulation results and discussion

To validate the proposed antenna, the configuration of Fig. 1 was then simulated in CST MWS. The simulated S_{11} parameter is depicted in Fig. 4. From the simulation, it is possible to observe that overall S11 antenna response (patch antenna plus transmitarray) presents a relatively good impedance matching, with bandwidth of 100MHz (S_{11}¡-10 dB) centered at 3.6 GHz. This simulation was considered

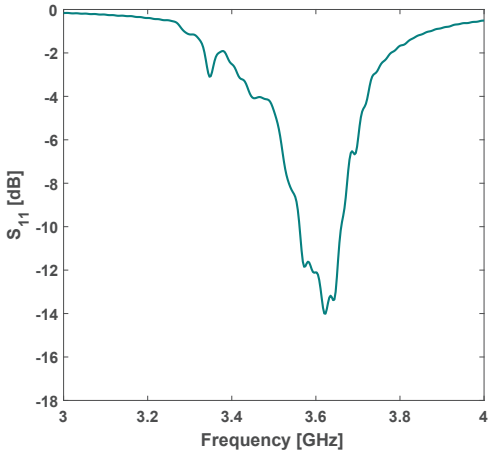

Fig. 4: Simulated S_{11} antenna matching.

when all the capacitance of the entire transmitarrray where set at 0.8 pF.

To validate the beamsteering capability, the beam steered angles were obtained by specifically defining the capacitance value of each element of the 5×5 transmitarray, according to the phase pattern defined by capacitance matrix previously calculated. In particular, the antenna was set to steer main lobe of the radiation pattern in both azimuth and elevation planes, independently. Two-dimensional radiation patterns are presented to evaluate the antenna performance.

According to the simulations results of Fig. 5, the antenna presents a maximum gain of 13.9 dBi when at boresight (0°,0°), against 18 dBi achieved with the microstrip array alone, which reflects the 4 dB of insertion loss caused by the transmitarray. Moreover, it is possible to observe that the antenna has the capability of performing beamsteering in a range defined 0° and 20°, in both azimuth (5a) and elevation planes (5b), without major deformation of the original main lobe. Although simulations are only presented for an angular sweep in the positive part of the axis, the antenna presents a good symmetry around the Y-axis in both antenna planes, with a maximum achievable angle of ±20°. Within the presented steering range, the maximum gain only decays of around 3 dB. For larger values, relatively high side lobes, with side lobe levels >7 dB start to appear.

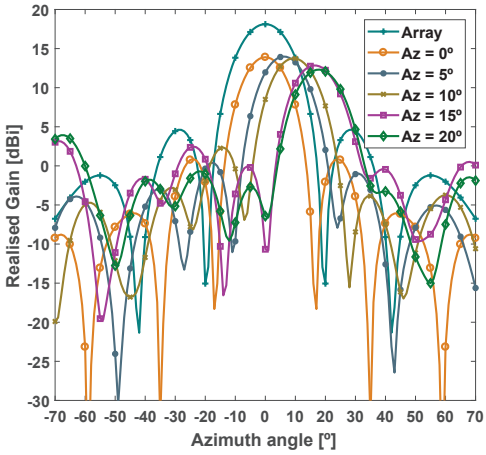

(a)

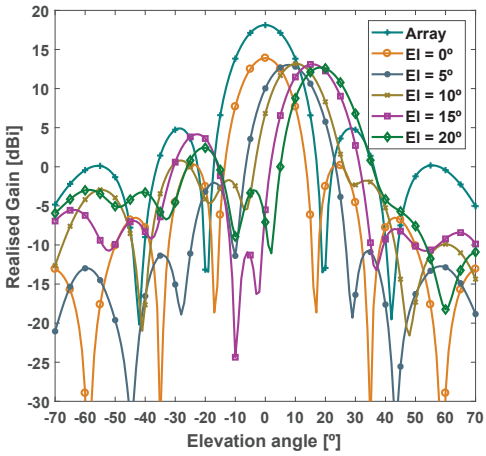

(b)

Fig. 5: Simulated output angular sweep in the (a) azimuth and (b) elevation planes, respectively.

V. Conclusions

This paper presents a novel flat-beamsteering antenna for 5G applications in the 3.6 GHz frequency bands. The proposed antenna presents a multi-layer structure composed of a microstrip patch array and a metamaterial inspired transmitarray structure that enables 2D-dimensional beamsteering, which replace the costly and complex phase-shifter networks. The proposed antenna presents in simulations 13.9 dBi of gain, 100 MHz of effective bandwidth with a maximum beamsteering range defined between ±20°, achievable in both elevation and azimuth planes, independently. Besides its good performance, the proposed antenna also presents a unique compact and flat form factor with a moderate size and appellative shapes, which allows the easy deployment whilst reduction the visual impact in 5G dense scenarios, when comparing with traditional base-station antenna.

Acknowledgment

This research was partially supported by FCT under the project WSN-EN: PTDC/EEI-EEE/30539/2017 and by FCT/MCTES through national funds and when applicable, co-funded EU funds under the project UIDB/EEA/50008/2020.

References

[1] A. Ghosh, A. Maeder, M. Baker, and D. Chandramouli, "5G Evolution: A View on 5G Cellular Technology Beyond 3GPP Release 15," *IEEE Access*, vol. 7, pp. 127 639–127 651, 2019.

[2] D. Muirhead, M. A. Imran, and K. Arshad, "A Survey of the Challenges, Opportunities and Use of Multiple Antennas in Current and Future 5G Small Cell Base Stations," *IEEE Access*, vol. 4, pp. 2952–2964, 2016.

[3] M. J. Marcus, "The Growing Visual Impact of Wireless Antennas in the Urban Landscape: Strategies for Coexistence," *IEEE Wireless Communications*, vol. 15, pp. 72–75, 2018.

[4] H. Huang, "Overview of Antenna Designs and Considerations in 5G Cellular Phones," in *2018 International Workshop on Antenna Technology (iWAT)*, March 2018, pp. 1–4.

[5] Y. Huo, X. Dong, W. Xu, and M. Yuen, "Cellular and WiFi Co-design for 5G User Equipment," in *2018 IEEE 5G World Forum (5GWF)*, July 2018, pp. 256–261.

[6] A. Zhao and Z. Ren, "Size Reduction of Self-Isolated MIMO Antenna System for 5G Mobile Phone Applications," *IEEE Antennas and Wireless Propagation Letters*, vol. 18, no. 1, pp. 152–156, Jan 2019.
[7] C. Sim, H. Liu, and C. Huang, "Wideband MIMO Antenna Array Design for Future Mobile Devices Operating in the 5G NR Frequency Bands n77/n78/n79 and LTE Band 46," *IEEE Antennas and Wireless Propagation Letters*, vol. 19, no. 1, pp. 74–78, Jan 2020.
[8] Y. Liu, S. Wang, N. Li, J. Wang, and J. Zhao, "A Compact Dual-Band Dual-Polarized Antenna With Filtering Structures for Sub-6 GHz Base Station Applications," *IEEE Antennas and Wireless Propagation Letters*, vol. 17, no. 10, pp. 1764–1768, Oct 2018.
[9] Q. Jia, H. Xu, M. F. Xiong, B. Zhang, and J. Duan, "Omnidirectional Solid Angle Beam-Switching Flexible Array Antenna in Millimeter Wave for 5G Micro Base Station Applications," *IEEE Access*, vol. 7, pp. 157 027–157 036, 2019.
[10] W. Chen, H. Lin, H. Ding, Y. Liu, M. Chisala, Z. Shen, H. Zhibin, L. Baihui, and R. Wang, "A Low Profile Broadband Dual-Polarized Base Station Antenna Using Folded Dipole Radiation Element," *IEEE Access*, vol. 7, pp. 67 679–67 685, 2019.
[11] J. R. Reis, N. Copner, A. Hammoudeh, Z. M. E. Al-Daher, R. F. S. Caldeirinha, T. R. Fernandes, and R. Gomes, "FSS-Inspired Transmitarray for Two-Dimensional Antenna Beamsteering," *IEEE Transactions on Antennas and Propagation*, vol. 64, no. 6, pp. 2197–2206, June 2016.
[12] J. R. Reis, R. F. S. Caldeirinha, A. Hammoudeh, and N. Copner, "Electronically Reconfigurable FSS-Inspired Transmitarray for 2-D Beamsteering," *IEEE Transactions on Antennas and Propagation*, vol. 65, no. 9, pp. 4880–4885, Sept 2017.
[13] M. Vala, J. R. Reis, and R. F. S. Caldeirinha, "A 28 GHz Fully 2D Electronic Beamsteering Transmitarray for 5G and future RADAR applications," in *Loughborough Antennas & Propagation Conference 2018 (LAPC 2018)*, 2018.
[14] C. A. Balanis, *Antenna Theory: Analysis and Design, 3rd Edition*. John Wiley & Sons, 2005, vol. 72.
[15] A. Bhattacharyya, *Phased Array Antennas: Floquet Analysis, Synthesis, Bfns and Active Array Systems*, ser. Wiley Series in Microwave and Optical Engineering. Wiley, 2006.
[16] B. A. Munk, *Frequency Selective Surfaces: Theory and Design*. John Wiley & Sons, 2005.